Smart Structures and Systems, *Vol. 35, No. 6 (2025) 305-314*
https://doi.org/10.12989/sss.2025.35.6.305

Genetic algorithm-based optimization of a tuned inerter damper for structural seismic response reduction

Ayman Nasir [1], Raed AlSaleh*[2], Alia Mahmoud [1], Omar Omar [3] and Ahmad Manasrah [1]

[1] *Department of Mechanical Engineering, Al-Zaytoonah University of Jordan, Amman, Jordan*
[2] *Department of Civil and Environmental Engineering, German Jordanian University, Amman, Jordan*
[3] *Department of Mechanical Engineering, Al Hussein Technical University, Amman, Jordan*

(*Received June 17, 2025, Revised June 20, 2025, Accepted June 24, 2025*)

Abstract. This research examines a model of a Tuned Inerter Damper (TID) developed by the authors in minimizing vibrations in a five-story structure when exposed to seismic activity. The TID model is developed using MATLAB Simulink and tested on a 5-story building model when exposed to an earthquake signal. The TID model configurations were calibrated to match the primary vibration frequency of the building using established tuning approaches. Then, genetic algorithm optimization was employed to enhance the inertance parameter for better performance under earthquake excitation throughout all building levels. Time-based simulations were performed comparing different scenarios with the TID optimized system. The results demonstrated that implementing the developed model of TID lead to substantial reductions in vibration magnitudes over time, which confirmed the potential of the inerter in enhancing structural oscillations control.

Keywords: frequency response; genetic algorithm; passive inerter; tuned inerter damper; vibration mitigation

1. Introduction

Traditional passive control devices, such as tuned mass dampers (TMDs), have been widely investigated in literature on several types of structures and proved sufficient in enhancing vibration mitigation, like; multi-story buildings (Yang *et al*. 2022), suspension bridge towers (Casciati and Giuliano 2009), and footbridges (Bortoluzzi *et al*. 2015). These control devices have been also adopted in real structures due to their simplicity and cost-effectiveness; however, they often require large auxiliary masses and exhibit limited performance in multi-mode vibration conditions. To overcome these limitations, recent studies have introduced inerter-based mechanical devices capable of generating a large apparent mass using relatively small physical components offering a promising solution to enhance vibration mitigation without increasing structural weight (Chen *et al*. 2021). Among these, the Tuned Inerter Damper (TID) has emerged as an effective alternative, extending the classical TMD by incorporating an inerter element to amplify damping performance while maintaining practical design feasibility (Jangid 2022).

An early application of TIDs incorporating pendulum-type TMD installed in Osaka's Crystal Tower reduced wind-induced motion by 50%, (Nagase and Hisatoku 1992). In parallel, semi-active systems emerged as a practical alternative, offering efficiency with reduced force demands (Symans and Constantinou 1999). While, Soong and Spencer (2002) highlighted the integration of smart devices and adaptive damping technologies, which marked a shift toward intelligent structural control.

Optimization of TMD parameters, such as the mass ratio, is critical for achieving maximum efficiency. Accordingly, Bekdaş and Nigdeli (2013) highlighted that conventional formulas may fall short in certain conditions, advocating for metaheuristic algorithms such as Harmony Search to fine-tune TMD properties for different structures and various excitations. To enhance control performance further, Tuned Mass Damper Inerter (TMDI) systems have emerged. These devices combine classical TMDs with inerters, which significantly increase apparent mass and energy dissipation. Pietrosanti *et al*. (2017) investigated various optimization strategies for TMDI systems and confirmed their superiority over traditional TMDs in reducing displacement and acceleration responses.

Recent works have focused on hybrid configurations and nonlinear optimization. Masnata *et al*. (2021) assessed the effectiveness of TMDIs in base-isolated structures and showed better control of displacement compared to TMDs. While, Rajana *et al*. (2023) introduced a nonlinear viscous damper into TMDI configurations, which optimized the damping behavior under seismic loads. Andditionally, Patsialis *et al*. (2023) evaluated multi-story hysteretic buildings using a reduced-order model and a bi-objective framework that balances drift suppression and force efficiency, confirming that TMDIs maintain high performance even under nonlinear behavior.

Inerter-based configurations have increasingly explored by researched to further improve structural control performance (Gao *et al*. 2021 and Cao *et al*. 2020). In bridge engineering, Sun *et al*. (2017) demonstrated the

*Corresponding author, Ph.D., Professor,
E-mail: raed.alsaleh@gju.edu.jo

ISSN: 1738-1584 (Print), 1738-1991 (Online)

efficiency of combining Tuned Inerter Dampers (TIDs) with cable networks to improve multi-mode vibration control in stay cables. While in building applications, Ruiz *et al*. (2018) explored a risk-informed optimization approach for TMDIs, showing they reduce seismic responses and lower life cycle and repair costs. Similarly, Taflanidis *et al*. (2019) introduced a multi-objective framework to balance vibration suppression and control force demands in inerter-based configurations, emphasizing real-world deployment constraints. In further studies, efforts have focused on adaptive structures, where inerters are combined with negative stiffness devices to effectively target multiple vibration modes (Irakoze *et al*. 2023). Nagarajaiah *et al*. (2022) highlighted this strategy as an effective approach to achieve frequency-independent damping across several structural modes. Finally, review studies such as that by Ma *et al*. (2021) confirm that inerter-based devices are a promising direction for cost-effective and scalable vibration mitigation in modern engineering systems.

On the other hand, Genetic Algorithms (GA) have emerged as a powerful optimization tool in various applications (Jaradat *et al*. 2022), among which, the design of TMD and TMDI systems for controlling structural vibrations under seismic and wind loads. Pandit *et al*. (2024) proposed a GA-based framework to minimize top-floor displacement in multi-degree-of-freedom (MDOF) buildings, evaluating the performance of TMDIs under real earthquake records. Colherinhas *et al*. (2019) also applied a GA to optimize pendulum TMDs in high-rise towers, focusing on minimizing frequency peaks by tuning parameters like pendulum length and mass ratio. Furthermore, Djerouni *et al*. (2020) introduced a double-mass TMDI scheme optimized via GA, which showed significant reductions in peak displacement, acceleration, and energy under both near- and far-fault ground motions. While, Pan *et al*. (2022) enhanced GA performance through a modified differential crossover strategy to maximize energy dissipation efficiency in inerter systems.

Despite extensive research on vibration control using TMD and TMDI systems, there are still significant gaps in the existing literature. Many previous studies have relied on simplified analytical models or simulations without applying their findings to real structures. Additionally, some have optimized system parameters using general metaheuristic methods but have not incorporated these optimizations into practical, implementable systems. While the advantages of inerter-based systems are well recognized, few studies utilize MATLAB Simulink for detailed simulation and time-domain analysis of multi-story buildings equipped with TIDs. Even fewer combine genetic algorithm optimization with physical modeling in case studies involving actual buildings. These shortcomings highlight the need for a comprehensive approach that merges advanced optimization techniques with practical system implementation. This study's novelty lies in applying a TID system to a real five-story building subjected to El-Centro seismic excitation, employing MATLAB Simulink for dynamic modeling and detailed floor-by-floor response assessment, and optimizing TID parameters using a genetic algorithm to minimize vibration amplitude, with the goal of future validation through targeted experimental testing.

Fig. 1 The Kajima-Shizuoka Building

Table 1 Computed modal properties from modal analysis of the uncontrolled building

Floor	Mass (kg)	Stiffness (kN/m)
1st floor	215.2×10^3	147×10^3
2nd floor	209.2×10^3	113×10^3
3rd floor	207.0×10^3	99×10^3
4th floor	204.8×10^3	89×10^3
5th floor	266.1×10^3	84×10^3

2. Design and methodology

Herein, a tuned inerter damper is installed within the model of Kajima-Shizuoka Building, the case-study building that consists of five stories and located in Japan, Fig. 1. Table 1 lists the mass and stiffness parameters for each story of the building. These parameters were incorporated into the model for an accurate representation of the structure's dynamic response to seismic excitations. According to literature, a TID demonstrated effective performance when placed at the bottom of the structure (Abd-Elhamed and Alkhatib 2023). Therefore, the TID was placed between the ground level and the first story in the simulation model.

In this research, the well-documented El Centro

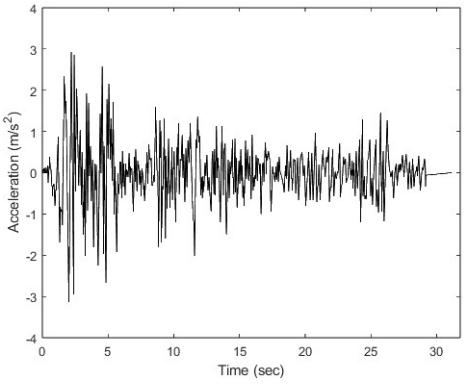

Fig. 2 Acceleration record of the 1940 El Centro earthquake used for dynamic loading simulations

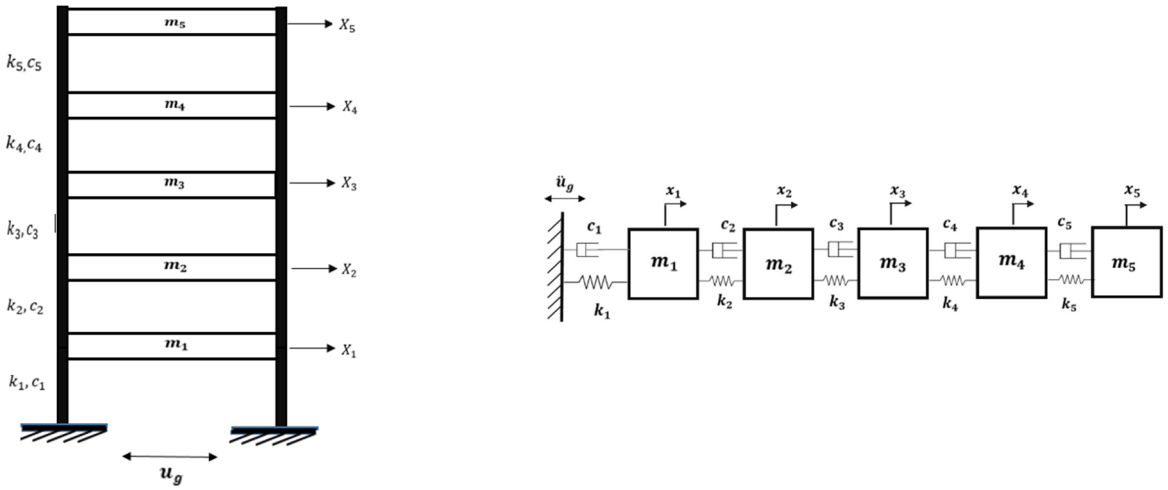

(a) 5-DoF uncontrolled multi-story building structure (b) Base-excited mechanical system model

Fig. 3 Five-story building using lumped mass and spring-damper elements representation

earthquake was chosen as the primary excitation signal for the building model in MATLAB Simulink. This seismic event is widely studied and can be considered as a valuable input to simulate real world scenarios. The acceleration time history corresponding to the El Centro earthquake is shown in Fig. 2. By integrating this acceleration signal into our model, accurate data about the response of the structure shall be expected.

2.1 Mathematical model for uncontrolled structure

One A schematic representation for the five-story structure subjected to base excitation $(\ddot{u}_g)$ is shown in Fig. 3(a). The system is modelled as a 5-Degrees-of-Freedom (DoF) system in which each story responds with a unique horizontal displacement. The stiffness and damping characteristics of each story are represented by k and c. Moreover, Fig. 3(b) illustrates the equivalent five degrees of freedom base excited mass-spring-damper system.

The equations of motion of the 5-DoF system were derived using Newton's second law as

$$\begin{aligned}
&m_1\ddot{x}_1 + (c_1 + c_2)\dot{x}_1 - c_2\dot{x}_2 + (k_1 + k_2)x_1 - k_2x_2 = -m_1\ddot{u}_g \\
&m_2\ddot{x}_2 + (c_2 + c_3)\dot{x}_2 - c_3\dot{x}_3 - c_2\dot{x}_1 + (k_2 + k_3)x_2 - k_2x_1 - k_3x_3 = -m_2\ddot{u}_g \\
&m_3\ddot{x}_3 + (c_3 + c_4)\dot{x}_3 - c_4\dot{x}_4 - c_3\dot{x}_2 + (k_3 + k_4)x_3 - k_3x_2 - k_4x_4 = -m_3\ddot{u}_g \\
&m_4\ddot{x}_4 + (c_4 + c_5)\dot{x}_4 - c_5\dot{x}_5 - c_4\dot{x}_3 + (k_4 + k_5)x_4 - k_4x_3 - k_5x_5 = -m_4\ddot{u}_g \\
&m_5\ddot{x}_5 + c_5\dot{x}_5 - c_5\dot{x}_4 + k_4x_4 - k_3x_2 = -m_5\ddot{u}_g
\end{aligned} \tag{1}$$

The generalized mathematical model for the 5-DoF structure can be described in matrix form as following

$$\boldsymbol{M\ddot{x} + C\dot{x} + Kx = -Mr\ddot{u}_g} \tag{2}$$

Where $\boldsymbol{x} = [x_1, x_2, x_3, x_4, x_5]^T$ and $r = [1,1,1,1,1]^T$ are the displacement and influence vectors in generalized coordinates. The generalized mass, damping and stiffness are expressed as 5 × 5 matrices and are denoted by M, C and K, respectively.

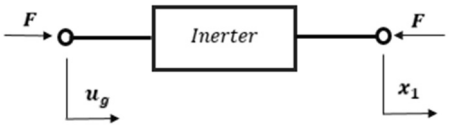

Fig. 4 Conceptual diagram of an inerter illustrating its force-velocity relationship between terminals

2.2 The mechanical inerter

A mechanical inerter has the ability to generate an inertial force directly proportional to the relative displace ement across its two terminals as shown in Fig. 4.

The constant of proportionality is known as the inertance (b) and is measured in kilograms. For a multistory structure equipped with a mechanical inerter between the base and the first story, the Force generated by the inerter (F_b) can be expressed as

$$F_b = b(\ddot{x}_1 - \ddot{u}_g) \tag{3}$$

2.3 Mathematical model for TID controlled structure

Fig. 5(a) shows a schematic representation for a TID controlled building structure subjected to base excitation $(\ddot{u}_g)$. The TID is inserted between the base and the first story. With the implementation of a TID, the structure is now modelled as a 6-DoF system. In addition to the horizontal displacement of each story, the Inerter responds to base excitation $(\ddot{u}_g)$ by a horizontal displacement (x_d) which is the relative displacement across its two terminals. The equivalent 6-DoF spring-mass-damper system is

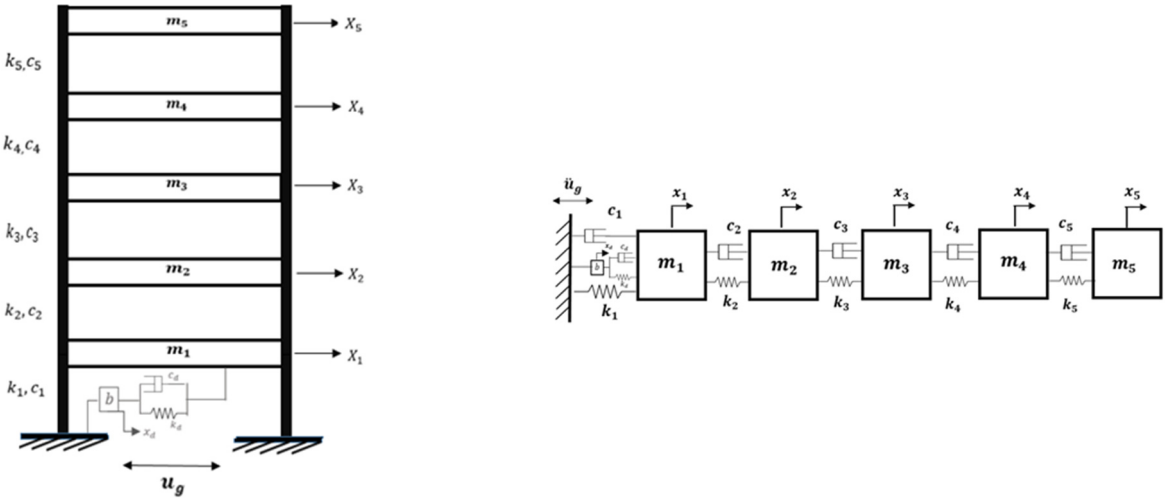

(a) 6-DoF controlled multi-story building structure (b) Base-excited mechanical system model

Fig. 5 Modified 6-DoF system including the TID connected between the ground and first floor

illustrated in Fig. 5(b).

The equations of motion of the 6-DoF system were derived using Newton's second law as

$$\begin{aligned}
&m_1\ddot{x}_1 + (c_1 + c_2 + c_d)\dot{x}_1 - c_2\dot{x}_2 + (k_1 + k_2 + k_d)x_1 - k_2x_2 - k_dx_d - c_d\dot{x}_d = -m_1\ddot{u}_g \\
&m_2\ddot{x}_2 + (c_2 + c_3)\dot{x}_2 - c_3\dot{x}_3 - c_2\dot{x}_1 + (k_2 + k_3)x_2 - k_2x_1 - k_3x_3 = -m_2\ddot{u}_g \\
&m_3\ddot{x}_3 + (c_3 + c_4)\dot{x}_3 - c_4\dot{x}_4 - c_3\dot{x}_2 + (k_3 + k_4)x_3 - k_3x_2 - k_4x_4 = -m_3\ddot{u}_g \\
&m_4\ddot{x}_4 + (c_4 + c_5)\dot{x}_4 - c_5\dot{x}_5 - c_4\dot{x}_3 + (k_4 + k_5)x_4 - k_4x_3 - k_5x_5 = -m_4\ddot{u}_g \\
&m_5\ddot{x}_5 + c_5\dot{x}_5 - c_5\dot{x}_4 + k_5x_5 - k_5x_4 = -m_5\ddot{u}_g \\
&b\ddot{x}_d - k_dx_1 + k_dx_d - c_d\dot{x}_1 + c_d\dot{x}_d = 0
\end{aligned} \tag{4}$$

Similarly, a generalized mathematical model for the 6-DoF structure can be described in matrix form as in Eq. (2), herein, as a result of the inclusion of the TID, the generalized mass, damping and stiffness are expressed as 6 × 6 matrices.

2.4 TID optimum parameters using fixed point theorem

The tuning methodology employed in this research is sourced from the research conducted by Lazar *et al*. (2013). In which, a fixed-point approach was used to formulate two sets of straightforward equations in order to obtain optimal damping and frequency ratios of the TID. The derivation of these parameters is based on the frequency response associated with the displacement response of the structure subjected to ground excitation. For a 5-DoF, the equivalent mass and stiffness for each mode were found using Eq. (2) and by targeting the first mode of vibration, the equivalent parameters for the first mode were used in the tuning procedure.

$$Meq_i = [\varphi]^T[M]r \tag{5}$$

When targeting the first mode of vibration, the system is reduced to 2-DoF as illustrated in Fig. 6, for which the equations of motion are given by

$$\begin{bmatrix} -\boldsymbol{M_{eq1}\omega^2 + K_{eq1}} & \boldsymbol{-b\omega^2} \\ \boldsymbol{-c_d\omega i - k_d} & \boldsymbol{-b\omega^2 + c_d\omega i + k_d} \end{bmatrix} \begin{bmatrix} \boldsymbol{x} \\ \boldsymbol{x_b} \end{bmatrix} = \begin{bmatrix} \boldsymbol{-M_{eq1}\ddot{u}_g} \\ \boldsymbol{0} \end{bmatrix} \tag{6}$$

The complex frequency response function representing the ratio of the structure's displacement to the ground acceleration amplitude is described in Eq. (7). Additionally, the FRF magnitude in dimensionless form is given Eq. (8).

Where $\lambda = \omega/\omega_1$ represents the ratio of excitation frequency to the natural frequency of the first mode; $\gamma = \omega_d/\omega_1$ represents the TID frequency ratio; $\mu = b/M_{eq1}$ denotes the inertance to structural mass ratio and $\zeta_d = c_d/2b\omega_d$ denotes the TID damping ratio.

By implementing the fixed-point theory, the optimal parameters for the TID in a single-DoF structure are as in Eqs. (9) and (10). (Lazar *et al*. 2013)

$$H_1(i\omega) = \frac{X}{\ddot{U}_g} = \frac{M_{eq1}[-c_d\omega + i(-b\omega^2 + k_d)]}{c_d\left[-(b + M_{eq1})\omega^3 + k_s\omega\right] + i[-bM_{eq1}\omega^4 + (k_db + k_dM_{eq1} + K_{eq1}b)\omega^2 - k_dK_{eq1}]} \tag{7}$$

$$|H_1(\lambda)| = \left|\frac{X}{\ddot{U}_g}\omega_1\right| = \sqrt{\frac{(-\lambda^2 + \gamma^2)^2 + (2\zeta_d\gamma\lambda)^2}{[\mu\lambda^2\gamma^2 - (\lambda^2 - 1)(\lambda^2 - \gamma^2)]^2 + [2\zeta_d\gamma\lambda(1 - (\mu + 1)\lambda^2)]^2}} \tag{8}$$

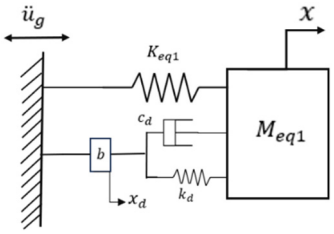

Fig. 6 2-DoF equivalent model used for fixed-point tuning of the TID

$$\gamma_{opt} = \frac{1}{\mu + 1} \tag{9}$$

$$\zeta_{d,opt} = \sqrt{\frac{3\mu}{8(\mu + 1)}} \tag{10}$$

2.5 Genetic algorithm

A population of 500 individuals was used in the GA, each representing a potential solution defined by three decision variables: inerter mass b, damping coefficient c_d, and spring stiffness k_d. These parameters directly influence the TID's effectiveness in reducing structural vibrations. The relatively large population size is chosen to enhance search space coverage, preserve genetic diversity, and to reduce the risk of premature convergence despite higher computational demands.

2.5.1 Constraints and design bounds

To ensure practical feasibility, upper bounds were imposed based on structural properties. The inerter mass was limited to 20% of the structure's equivalent mass (2.974×10^6 kg), and spring stiffness was capped at 10% of the structure's stiffness (5.9663×10^7 N/m). The upper limit for damping was derived using a damping ratio of 0.5. These bounds ensure the TID remains lightweight and suitable for real-world applications.

2.5.2 Objective function

The GA minimizes the peak absolute displacement of the structure under El Centro earthquake excitation. The TID parameters serve as inputs to a state-space model that simulates system dynamics, and the objective function returns the maximum displacement of the equivalent mass

$$F_V(b, c_d, k_d) = \max\left|q_{eq}(t)\right| \tag{11}$$

This formulation ensures the TID configuration delivers optimal vibration suppression.

2.5.3 Population sorting

Each individual is evaluated based on its objective function value. The population is sorted in ascending order of cost, allowing the best-performing solutions to dominate reproduction and survival.

2.5.4 Selection

A roulette wheel selection method assigns reproduction probabilities proportional to fitness, favoring better solutions while maintaining population diversity.

2.5.5 Crossover

Uniform crossover combines parent genes using a weighted average controlled by $\gamma = 0.1$, generating offspring with inherited traits that explore a broader solution space.

2.5.6 Mutation

To prevent stagnation, mutation introduces controlled randomness. With a probability of $\mu = 0.05$, genes are perturbed by normally distributed noise $\sigma = 0.1$, enabling exploration of new regions in the search space

3. Results and discussion

Modal analysis was conducted to find the dynamic characteristics of a vibrating MDOF system. This analysis yielded a set of natural modes for which each represents unique vibrational patterns that contribute to the overall response of the structure. For a 5-DoF system, there exists five different modes of vibration, each represented by a specific natural frequency, which implies that the structure would undergo resonance at five frequencies. Fig. 7 illustrates the five mode shapes. It visually represents the displacement patterns associated with distinct natural frequencies. The modal parameters including the modal mass and modal stiffness are summarized in Table 2.

Fig. 8 shows the magnitude of the frequency response in receptance form in addition to the phase. In the FRF graph, the five distinct peaks corresponding to each natural frequency are observed. These peaks represent the resonant frequencies at which the structure exhibits amplified response to the base excitation. It can be seen that the phase angle at each of the five peaks is 180°. This phase relationship signifies that the system's response is exactly

Table 2 Modal parameters of the 5-story building

Mode	Natural frequency (rad/s)	Mode shape	Modal mass (kg)	Modal stiffness (N/m)
1st Mode	6.3347	0.1958, 0.4356, 0.6723, 0.8729, 1.0000	563640	2.2618e+07
2nd Mode	17.7475	-0.6874, -1.1694, -0.9411, 0.0022, 1.0000	837210	2.6370e+08
3rd Mode	28.2295	1.4194, 1.1118, -1.1116, -1.5245, 1.0000	1690000	1.3468e+09
4th Mode	36.4262	-2.6320, 0.5949, 2.6101, -3.2033, 1.0000	5342700	7.0891e+09
5th Mode	42.5594	12.0646, -13.8574, 9.5944, -4.7379,1.0000	95414000	1.7282e+11

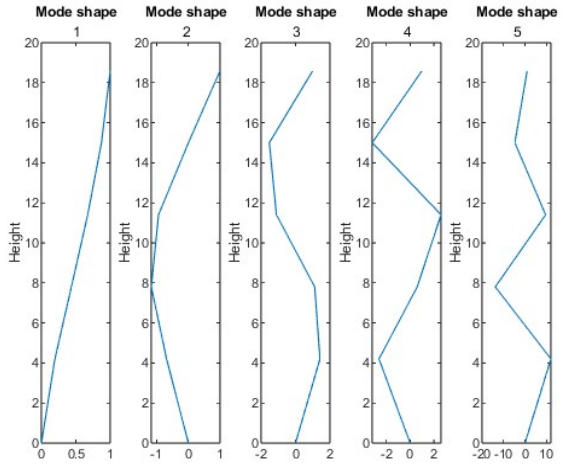

Fig. 7 Mode shapes of the five-story building extracted from modal analysis

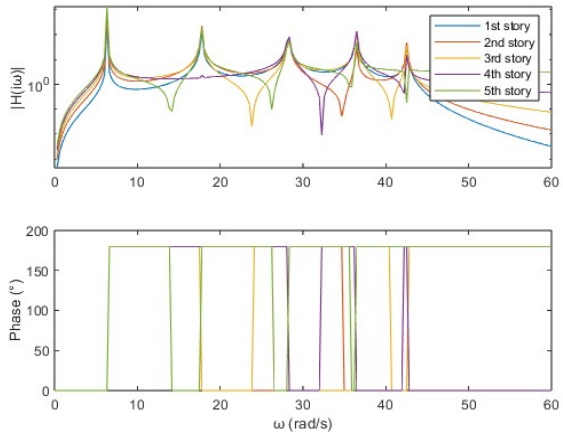

Fig. 8 Frequency response and phase plot of the uncontrolled building system

out of phase with the applied excitation. It is noteworthy to mention that using a linear scale in FRF magnitude curve can make certain details such as anti-resonances invisible since the curve is swamped. However, when utilizing a logarithmic scale, a more detailed view of the entire FRF curve is evidenced.

3.1 TID tuning

In this work, the equivalent mass and stiffness for each mode was found using Eq. (5) and by targeting the first mode of vibration, the equivalent parameters for the first mode were used in the tuning procedure. In this section, the results of the tuning process are presented in Table 3. It is worth noting that the inertance to structural mass ratio was set to 0.25.

Fig. 9 presents the FRF for the first mode, it can be seen that FRFs of different TID damping ratios pass through the same two points. However, for the optimum damping ratio value, at least one of the two intersection points has a gradient of zero. It can also be noticed that for all values of ζ_d the response significantly decreased and a new peak was introduced. Both peaks are shifted away from the targeted

Table 3 Optimized TID parameters obtained through the fixed-point approach

Inertance-to-structural-mass-ratio (μ)	0.25
Inertance (b) (kg)	179320
Optimum TID frequency ratio (γ_{opt})	0.8
Optimum damping ratio ($\zeta_{d,opt}$)	0.2739
Optimum damping coefficient (c_d) (Ns/m)	497750
Optimum Stiffness (k_d) (N/m)	4605400

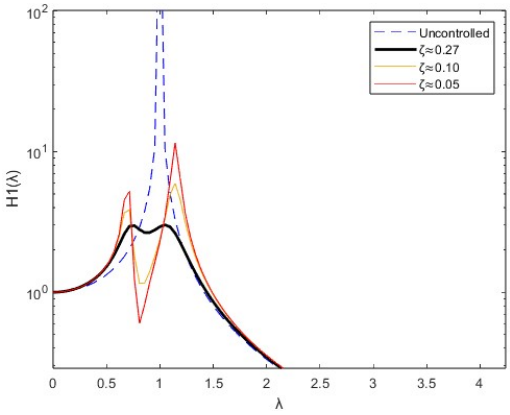

Fig. 9 Effect of varying damping ratios on the frequency response function of the first mode

resonant frequency. The FRF magnitude was plotted against excitation frequency for each of the modes. This was done by finding the equivalent parameters for each mode and treating them individually as a single-DoF system with a TID. The optimum TID parameters presented earlier were used for all modes. It can be shown that even through targeting one vibrational mode, other modes are affected as well. This can be seen through the reduced frequency response in all modes. However, despite the reduced response, the peak was only shifted in the first mode.

In Fig. 10, the FRF magnitude was plotted against excitation frequency for each of the modes. This was done by finding the equivalent parameters for each mode and treating them individually as a single-DoF system with a TID. The optimum TID parameters presented earlier were used for all modes.

3.2 Time response

The time history graphs, in Fig, 11, illustrate the dynamic response for each story before and after the implementation of the TID. Before the TID, the time displacement graphs show relatively large responses to the external seismic excitation. However, after the incorporation of a TID, A notable reduction in amplitude is evident. The system's response becomes damped with a quicker decay. Another observation is that as time progresses, the most significant decrease in amplitude becomes increasingly evident. It is also clear that the roof of the structure exhibited largest dynamic response amplitude when compared to the other stories.

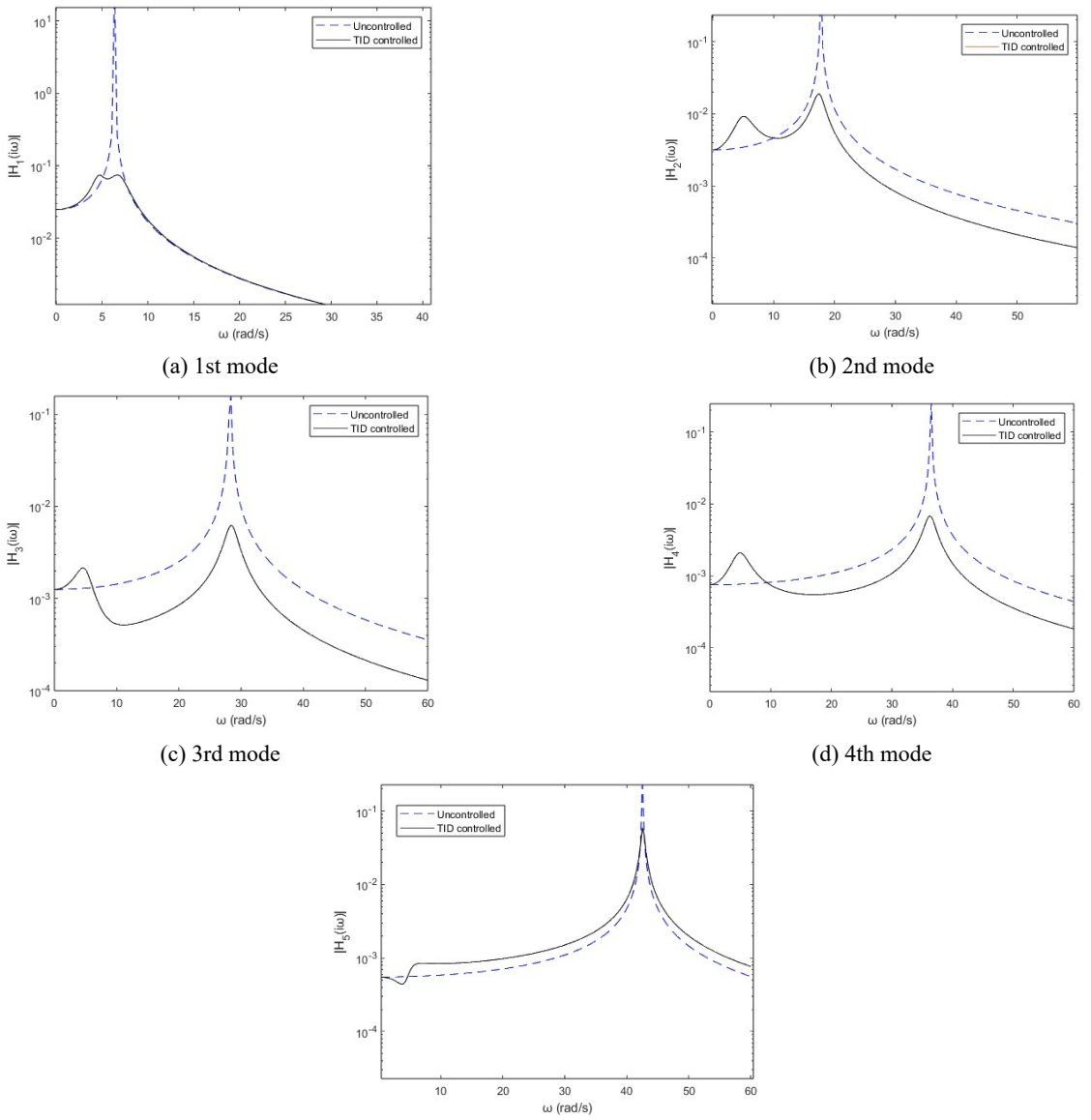

(a) 1st mode

(b) 2nd mode

(c) 3rd mode

(d) 4th mode

(e) 5th mode

Fig. 10 Frequency response for the first 5 modes of the structure using fixed-point-tuned TID

3.3 GA optimization results

The application of the GA in this study provided an effective mechanism for optimizing the key parameters of the TID system: inertance, damping coefficient, and stiffness, the optimized results are shown in Table 4. These optimized values obtained were significantly higher than those derived through the fixed-point method (Table 3), indicating that the GA was able to explore a broader and more complex design space beyond the simplified assumptions inherent in traditional tuning approaches.

The optimized inertance value increased by nearly an order of magnitude compared to the fixed-point value (from 179,320 kg to 1.76 × 10^6 kg), suggesting that a more substantial inertial contribution is beneficial for mitigating vibration in this particular structure. Similarly, both the damping coefficient and stiffness were elevated, aligning with the goal of achieving faster energy dissipation and greater structural control under seismic excitation.

Table 4 Optimized TID parameters obtained using the GA approach

Inertance (b) (kg)	1.7605 × 10^6
Optimum damping coefficient (c_d) (Ns/m)	3.7431 × 10^6
Optimum Stiffness (k_d) (N/m)	5.9084 × 10^7

The performance benefits of this optimization are evident in the displacement reduction across all floors. The first floor experienced a 62.03% peak displacement reduction, while the top floor (5th story) observed a 43.25% reduction, Table 5 shows the reduction percentages of all floors. This non-uniform distribution highlights the ability of the GA-optimized TID to effectively mitigate both local and global dynamic responses, despite being placed only between the ground and first story. This further underlines the TID's influence on higher vibrational modes, despite the optimization objective focusing on minimizing displacement

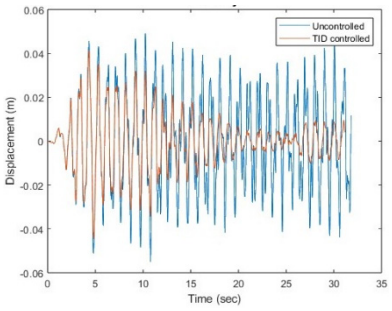

(a) 1st story

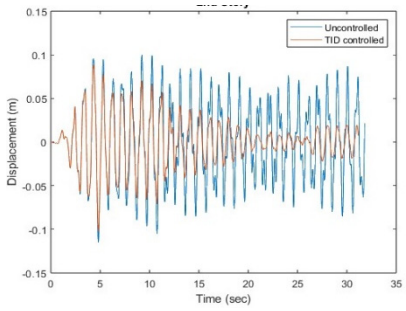

(b) 2nd story

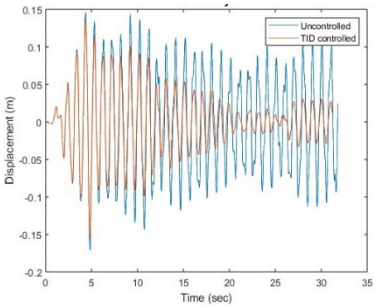

(c) 3rd story

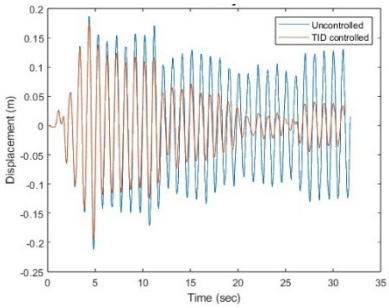

(d) 4th story

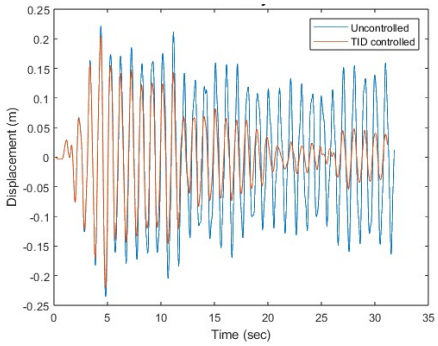

(e) 5th story

Fig. 11 Time-domain displacement response of all floors with and without TID under seismic loading

globally.

Overall, the GA-enabled optimization not only improved vibration suppression across all floors but also validated the benefit of using metaheuristic techniques for parameter tuning in structural control applications. The results reinforce the practical viability of implementing such algorithms in conjunction with simulation-based modelling platforms like MATLAB Simulink.

When compared to the response obtained using parameters derived from the fixed-point method, the GA-optimized values resulted in significantly greater reductions in displacement across all floors, as illustrated in Fig. 12. This confirms the limited enhancement of TID by traditional tuning strategies like the fixed-point technique, which are often restricted to modal assumptions and narrow design targets. While, the GA provided more flexible and comprehensive optimization framework that accounts for the structure's full dynamic behaviour under seismic loading. This highlights the advantage of GA, and its suitability for real-world structural response optimization, specially, where multiple performance objectives and constraints must be simultaneously satisfied.

4. Conclusions

This study highlighted the effectiveness of using a Genetic Algorithm (GA) for optimizing the design of a passive Tuned Inerter Damper (TID) aimed at reducing vibrations in a multi-story building. By applying GA, the optimal values for inerter mass, damping coefficient, and stiffness were determined, resulting in notable reductions in peak displacements throughout all floors of the building. The optimized TID achieved displacement reductions between 43.25% and 62.03%, demonstrating the GA's capability to significantly reduce structural vibrations during seismic events

The GA played a crucial role in the optimization process by enabling the identification of the best parameter combinations that minimized displacement responses. The use of GA facilitated the handling of complex dynamic interactions in multi-degree-of-freedom systems, providing an efficient approach for vibration mitigation. Additionally, the study confirmed that the GA-based optimization process outperforms traditional methods by offering a more flexible and reliable solution in real-world structural scenarios.

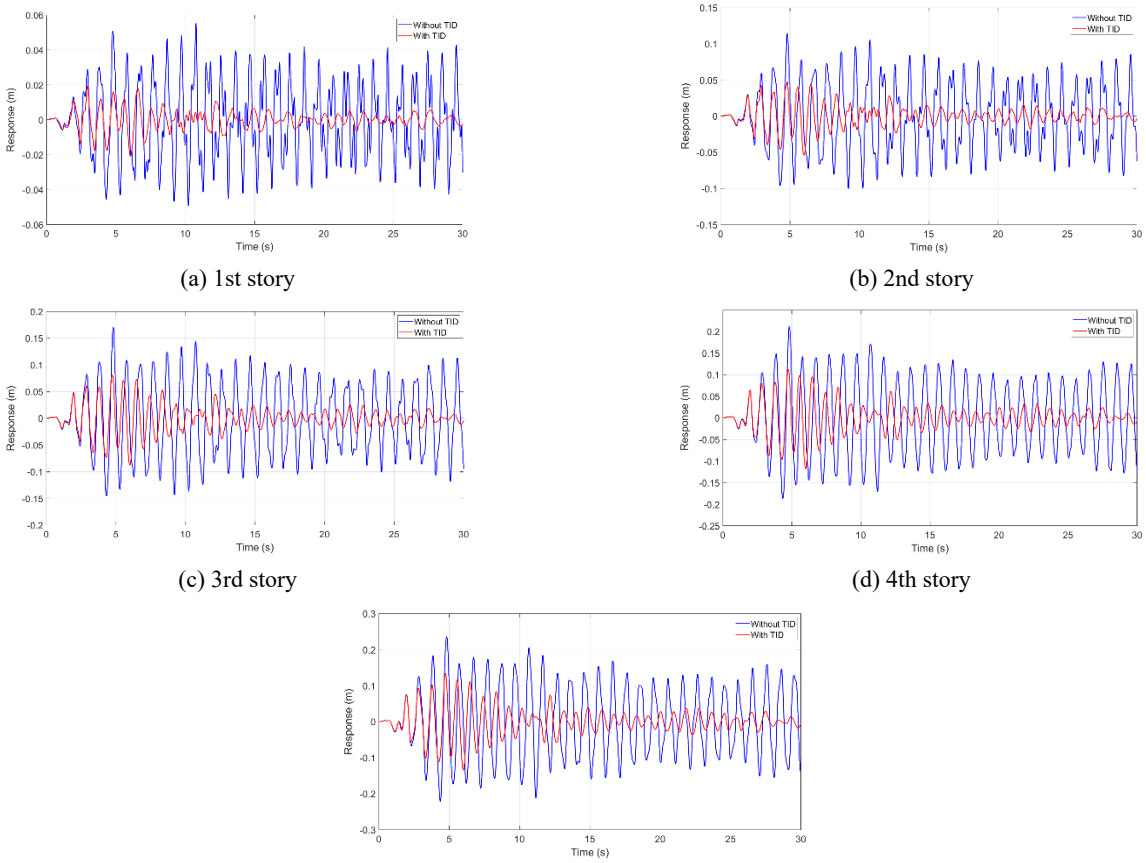

(a) 1st story

(b) 2nd story

(c) 3rd story

(d) 4th story

(e) 5th story

Fig. 12 Comparison of peak displacement across floors before and after applying the GA-optimized TID

Table 5 Percentage reduction in peak displacement on each floor using the GA-optimized TID

Floor number	Percentage reduction in peak displacement
1	62.03
2	52.85
3	49.00
4	44.32
5	43.25

The combination of GA optimization with time-history simulations and modal analysis yielded promising results, underscoring the potential of GAs for advanced vibration control in modern engineering systems. The findings of this research pave the way for the broader application of GA in the design of vibration control systems for tall buildings and other civil engineering structures subjected to dynamic excitations.

Finally, while the traditional fixed-point method provided a useful baseline for TID tuning by targeting the first vibrational mode, it offered limited control over higher modes and global structural behavior. In contrast, the GA successfully identified parameter sets that demonstrated superior performance for vibration mitigation across all floors.

Acknowledgments

This study was funded by Al-Zaytoonah University of Jordan under grant number 31/08/2023-2024 for the research project of the first author.

References

Abd-Elhamed, A. and Alkhatib, S. (2023), "Analytical solution of seismic responses of multi-storey building structures controlled by tuned mass-damper-inerter (TMDI)", *Eng. Sci.*, **26**, p. 963. https://doi.org/10.30919/es963

Bekdaş, G. and Nigdeli, S.M. (2013), "Mass ratio factor for optimum tuned mass damper strategies", *Int. J. Mech. Sci.*, **71**, 68-84. https://doi.org/10.1016/j.ijmecsci.2013.03.014

Bortoluzzi, D., Casciati, S., Elia, L. and Faravelli, L. (2015), "Design of a TMD solution to mitigate wind-induced local vibrations in an existing timber footbridge", *Smart Struct. Syst., Int. J.*, **16**(3), 459-478. https://doi.org/10.12989/sss.2015.16.3.459

Casciati, F. and Giuliano, F. (2009), "Performance of multi-TMD in the towers of suspension bridges", *J. Vib. Control*, **15**(6), 821-847. http://doi:10.1177/1077546308091455

Cao, L., Li, C. and Chen, X. (2020), "Performance of multiple tuned mass dampers-inerters for structures under harmonic ground acceleration", *Smart Struct. Syst., Int. J.*, **26**(1), 49-61. https://doi.org/10.12989/sss.2020.26.1.049

Chen, Q., Zhao, Z. and Zhang, R. (2021), "An inerter-system chain and energy-based optimal control of adjacent single-

degree-of-freedom structures", *Smart Struct. Syst.*, *Int. J.*, **28**(2), 245-259. https://doi.org/10.12989/sss.2021.28.2.245

Colherinhas, G.B., De Morais, M.V.G., Shzu, M.A.M. and Avila, S.M. (2019), "Optimal pendulum tuned mass damper design applied to high towers using genetic algorithms: Two-DOF modeling", *Int. J. Struct. Stab. Dyn.*, **19**(10), p. 1950125. https://doi.org/10.1142/S0219455419501256

Djerouni, S., Ounis, A., Athamnia, B., Charrouf, M.E., Abdeddaim, M. and Djedoui, N. (2020), "Optimal seismic response using a passive tuned mass damper inerter (TMDI)", *J. Build. Mater. Struct.*, **7**(1), 51-59. https://doi.org/10.34118/jbms.v7i1.208

Gao, H., Wang, H., Li, J., Wang, Z., Ni, Y. and Liang, R. (2021), "Damping enhancement of the inerter on the viscous damper in mitigating cable vibrations", *Smart Struct. Syst.*, *Int. J.*, **28**(1), 89-104. https://doi.org/10.12989/sss.2021.28.1.089

Irakoze, J., Li, S., Pu, W., Nyangi, P. and Sibomana, A. (2023), "Optimization of base-isolated structure with negative stiffness tuned inerter damper targeting seismic response reduction", *Earthq. Struct.*, *Int. J.*, **25**(6), 399-415. https://doi.org/10.12989/eas.2023.25.6.399

Jaradat, Y., Masoud, M., Jannoud, I. and Zeidan, D. (2022), "Genetic Algorithm Energy Optimization in 3D WSNs with Different Node Distributions", *Intell. Automat. Soft Comput.*, **33**(2), 791-808. https://doi.org/10.32604/iasc.2022.024218

Jangid, R.S. (2022), "Optimum parameters and performance of tuned mass damper-inerter for base-isolated structures", *Smart Struct. Syst.*, *Int. J.*, **29**(4), 549-560. https://doi.org/10.12989/sss.2022.29.4.549

Lazar, I., Neild, S. and Wagg, D. (2013), "Using an inerter-based device for structural vibration suppression", *Earthq. Eng. Struct. Dyn.*, **43**(8), 1129-1147. https://doi.org/10.1002/eqe.2390

Ma, R., Bi, K. and Hao, H. (2021), "Inerter-based structural vibration control: A state-of-the-art review", *Eng. Struct.*, **243**, p. 112655. https://doi.org/10.1016/j.engstruct.2021.112655

Masnata, C., Di Matteo, A., Adam, C. and Pirrotta, A. (2021), "Assessment of the tuned mass damper inerter for seismic response control of base-isolated structures", *Struct. Control Health Monitor.*, **28**, p. e2665. https://doi.org/10.1002/stc.2665

Nagarajaiah, S., Chen, L. and Wang, M. (2022), "Adaptive stiffness structures with dampers: Seismic and wind response reduction using passive negative stiffness and inerter systems", *J. Struct. Eng.*, **148**(11), p. 04022179. https://doi.org/10.1061/(asce)st.1943-541x.0003472

Nagase, T. and Hisatoku, T. (1992), "Tuned-pendulum mass damper installed in crystal tower", *Struct. Des. Tall Build.*, **1**(1), 35-56. https://doi.org/10.1002/tal.4320010105

Pan, C., Yang, D. and Wang, H. (2022), "Optimization of inerter system for seismic response control based on a modified genetic algorithm with differential crossover strategy", *Adv. Mech. Eng.*, **14**(6), p. 16878132221106296. https://doi.org/10.1177/16878132221106296

Pandit, A., Ghiasi, R. and Malekjafarian, A. (2024), "On the optimization of tuned mass damper inerter (TMDI) systems for buildings subjected to real ground motions using slime mould algorithm", *Soil Dyn. Earthq. Eng.*, **179**, p. 108557. https://doi.org/10.1016/j.soildyn.2024.108557

Patsialis, D., Taflanidis, A.A. and Giaralis, A. (2023), "Tuned-mass-damper-inerter optimal design and performance assessment for multi-storey hysteretic buildings under seismic excitation", *Bull. Earthq. Eng.*, **21**, 1541-1576. https://doi.org/10.1007/s10518-021-01236-4

Pietrosanti, D., De Angelis, M. and Basili, M. (2017), "Optimal design and performance evaluation of systems with tuned mass damper inerter (TMDI)", *Earthq. Eng. Struct. Dyn.*, **46**(8), 1367-1388. https://doi.org/10.1002/eqe.2861

Rajana, K., Wang, Z. and Giaralis, A. (2023), "Optimal design and assessment of tuned mass damper inerter with nonlinear viscous damper in seismically excited multi-storey buildings", *Bull. Earthq. Eng.*, **21**, 1509-1539. https://doi.org/10.1007/s10518-022-01609-3

Ruiz, R., Taflanidis, A.A., Giaralis, A. and Lopez-Garcia, D. (2018), "Risk-informed optimization of the tuned mass-damper-inerter (TMDI) for the seismic protection of multi-storey building structures", *Eng. Struct.*, **177**, 836-850. https://doi.org/10.1016/j.engstruct.2018.08.074

Soong, T.T. and Spencer, B.F. (2002), "Supplemental energy dissipation: State-of-the-art and state-of-the-practice", *Eng. Struct.*, **24**(3), 243-259. https://doi.org/10.1016/S0141-0296(01)00092-X

Sun, L., Hong, D. and Chen, L. (2017), "Cables interconnected with tuned inerter damper for vibration mitigation", *Eng. Struct.*, **151**, 57-67. https://doi.org/10.1016/j.engstruct.2017.08.009

Symans, M.D. and Constantinou, M.C. (1999), "Semi-active control systems for seismic protection of structures: A state-of-the-art review", *Eng. Struct.*, **21**(6), 469-487. https://doi.org/10.1016/S0141-0296(97)00225-3

Taflanidis, A.A., Giaralis, A. and Patsialis, D. (2019), "Multi-objective optimal design of inerter-based vibration absorbers for earthquake protection of multi-storey building structures", *J. Frankl. Inst.*, **356**(15), 7754-7784. https://doi.org/10.1016/j.jfranklin.2019.02.022

Yang, F., Sedaghati, R. and Esmailzadeh, E. (2022), "Vibration suppression of structures using tuned mass damper technology: A state-of-the-art review", *J. Vib. Control*, **28**(5), 812-836. https://doi.org/10.1177/1077546320984305